

Two-Photon Decay of the 1.76-MeV  $0^+$  State of  $^{90}\text{Zr}$ 

Yasuyuki Nakayama

*Institute for Chemical Research and Radioisotope Research Center, Kyoto University, Kyoto, Japan*

(Received 27 March 1972)

Measurements of the probability and the energy distribution for the two-photon decay from the 1.76-MeV  $0^+$  first excited state to the  $0^+$  ground state of  $^{90}\text{Zr}$  have been performed using a sum-coincidence technique with an antidetector and large lead shields. This improved experimental technique made it possible to eliminate unfavorable coincident events which would disturb true events from the two-photon process. The ratio of two-photon decay to the sum of internal-pair decay and internal-conversion decay,  $T_{\gamma\gamma}/T_{\pi+e}$ , has been found to be  $(5.1 \pm 2.5) \times 10^{-4}$ . This value is larger than the upper limits reported recently by other workers, and not consistent with any values calculated based on existing theories. The energy spectrum of one of two photons has also been observed. This spectrum suggests reasonably that two-photon decay takes place as an  $(E1, E1)$  transition via giant-dipole-resonance states. A discussion of the theoretical significance of this study is given.

## I. INTRODUCTION

As the second-order process for the transition between two nuclear states, there may occur two-photon emission or simultaneous emission of two conversion electrons or of one conversion electron and one photon. This process has been treated theoretically by many workers<sup>1-11</sup> and for the past decade much effort has also been devoted to confirming its existence; especially a two-photon decay of the  $0^+ \rightarrow 0^+$  transition has been investigated experimentally with some nuclei,  $^{16}\text{O}$ ,  $^{40}\text{Ca}$ , and  $^{90}\text{Zr}$ . Among these nuclei, a two-photon transition in  $^{90}\text{Zr}$  has been a focus of experimental study for many workers,<sup>12-19</sup> since in this case a single-photon emission is forbidden and the source to be used can be prepared easily from commercially available  $^{90}\text{Sr}$  solution. However, there are as yet no convincing experimental data; the experimental values of this transition probability so far obtained, expressed by a ratio of the two-photon decay to a sum of internal-pair and internal-conversion decay,  $T_{\gamma\gamma}/T_{\pi+e}$ , lie scattered from  $2.3 \times 10^{-3}$  to  $8 \times 10^{-5}$ , as discussed in Sec. IV.

In the present work, a two-photon transition from the 1.76-MeV  $0^+$  first excited state to the  $0^+$  ground state in  $^{90}\text{Zr}$  has been studied experimentally to elucidate the nature of this transition and intermediate states involved. In this nucleus the first-order processes are internal-pair creation and internal conversion. Although the emission of two conversion electrons may occur as the second-order process in competition with the emission of two photons, we confined ourselves only to observe the latter process.

According to the second-order perturbation theory, the matrix element for two-photon transition

can be expressed by

$$-\sum \frac{\langle f | H | n \rangle \langle n | H | i \rangle}{E_n - E_i}, \quad (1)$$

where  $i$ ,  $f$ , and  $n$  refer to the initial, final, and intermediate states, respectively.  $H$  is the Hamiltonian, representing the interaction of the nucleus with the electromagnetic field. The summation is performed over all intermediate states  $n$ . The process may be interpreted as follows. An initial state with energy  $E_i$  emits a first photon with an energy  $\omega_1$ , being transformed into virtual states which lie above the initial state. A second photon with an energy  $\omega_2$  is then emitted in a transition to the final state with  $E_f$ . The energy spectrum of the emitted photons is expected to be continuous under the condition  $\omega_1 + \omega_2 = E_i - E_f$ .

In the nuclear transition  $j_i \rightarrow j_f$  having the multipolarities  $L_1$  and  $L_2$  for the two photons emitted simultaneously, the condition  $|j_i - j_f| \leq L_1 + L_2 \leq j_i + j_f$  is required. Since two-photon emission of the lowest order  $L_1 + L_2 = |j_i - j_f|$  is completely forbidden in the  $0^+ \rightarrow 0^+$  transition, there may predominate the simultaneous emission of two photons with  $(E1, E1)$  and  $(M1, M1)$  competing with the emission of one conversion electron.  $(M1, M1)$  two-photon processes are, in general, smaller than  $(E1, E1)$  transitions by a factor  $10^4$ . Thus, in the present work only electric-dipole transitions need be considered. As an intermediate dipole state, the presence of the giant-dipole-resonance states of  $^{90}\text{Zr}$  has been confirmed experimentally. The angular correlation between two photons should be the same as two electric-dipole transitions in a  $0^+ \rightarrow 1^- \rightarrow 0^+$  cascade, in which the angular correlation function is  $1 + \cos^2\theta$ . For a  $0^+ \rightarrow 0^+$  transition the energy distribution of each of two photons is

approximately expressed<sup>8</sup> by  $W(\omega) \propto \omega^3(\omega_0 - \omega)^3$ , where  $\omega_0$  is the maximum energy of a continuous energy distribution in the two-photon decay and  $\omega$  is an energy of one of the two photons. Since the shape of an energy spectrum is sensitive both to the multiplicities of the two photons and the distribution of the intermediate states, information about these states can be obtained if one succeeds in measuring the energy distribution. In the present work, in addition to the measurement of the transition probability, the energy distribution has also been measured.

## II. EXPERIMENTAL ARRANGEMENT

The experimental method we adopted differs from those used by other workers<sup>12-19</sup> in that we introduced a  $\beta$ -ray detector (used as an antidetector) into the detector system of the sum-coincidence spectrometer. The anticoincidence device was adopted in order to eliminate absolutely the unfavorable coincidences due to the bremsstrahlung caused by  $\beta$  rays from the source. In the present work the energy distribution of two-photon decay and the sum-coincidence were measured simultaneously. Some details of the essential parts of the experimental method are described in the following subsections.

### A. Source

A  $^{90}\text{Y}$  source in radioactive equilibrium with  $^{90}\text{Sr}$ , at least 7 yr old at the beginning of this experiment, was used. The decay scheme of  $^{90}\text{Sr}$  is shown in Fig. 1. The 1.76-MeV  $2^+$   $0^+$  state of  $^{90}\text{Zr}$  with a half-life of 62 nsec<sup>21</sup> is populated by a 0.02%  $\beta$  branch with a maximum energy of the 0.51 MeV from 64-h  $^{90}\text{Y}$ .  $^{90}\text{Y}$  is fed by about 100%  $\beta$  de-

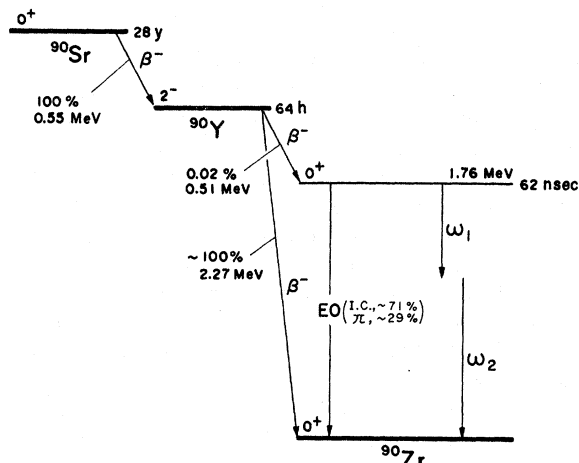


FIG. 1. Decay scheme of  $^{90}\text{Sr}$ .

cay of  $^{90}\text{Sr}$  which has a maximum energy of 0.55 MeV. The main branch of  $^{90}\text{Y}$  is the 2.27-MeV  $\beta$  decay to the  $0^+$  ground state of  $^{90}\text{Zr}$ . It should be noted that the two  $\beta$  rays having maximum energies of 0.55 MeV from  $^{90}\text{Sr}$  and of 2.27 MeV from  $^{90}\text{Y}$  produce intense bremsstrahlung in the neighborhood of the source.

To measure the very weak two-photon decay of the  $0^+ \rightarrow 0^+$  transition, it is required to get a source of extremely high purity and to know the degree of impurities which would affect the results of the experiment. The radioactive strontium chloride solution used in the present work was a standard product separated from fission products at Oak Ridge National Laboratory. According to analysis data from Oak Ridge,  $^{144}\text{Ce}$  impurity did not exceed  $6 \times 10^{-5}$  mCi/ml at the time of delivery. There are many  $\gamma$  rays from fission products having energies lying near 1.76 MeV of the first excited  $0^+$  state in  $^{90}\text{Zr}$ . In order to remove absolutely such impurities of fission products, if these exist, from the source, the original  $^{90}\text{Sr}$ - $^{90}\text{Y}$  solution was purified by ion exchange. Three exchange columns (1.0 cm diam by 40 cm long) packed with Dowex-50W X8, 100-200 mesh, were used. The  $^{90}\text{Sr}$ - $^{90}\text{Y}$  mixture was eluted through the first column with 1.0 M ammonium lactate solution (pH 5.1). The  $^{90}\text{Sr}$  fraction was again eluted through the second column with 10 N HCl. The  $^{90}\text{Sr}$  fraction from the second column was collected in a polypropylene beaker and evaporated to near dryness on a steam bath. Next, the  $^{90}\text{Sr}$  deposit was dissolved with a small amount of water, and was eluted through the third column with 3.0 N HCl. By the first elution,

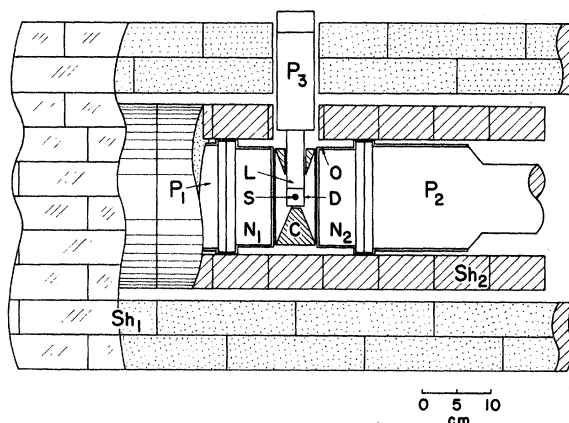


FIG. 2. Geometrical arrangement of detectors and lead shields;  $N_1$  and  $N_2$ , 127-mm-diam by 50-mm-thick NaI(Tl) crystals;  $D$ , plastic phosphor;  $L$ , Lucite light-guide pipe;  $S$ ,  $^{90}\text{Sr}$  source;  $P_1$  and  $P_2$ , RCA-4522 photomultiplier tubes;  $P_3$ , RCA-6810A photomultiplier tube;  $O$ , polyethylene cap;  $C$ , conical lead collimator;  $Sh_1$ , lead house;  $Sh_2$ , lead ring.

alkali and alkaline earth metals, heavy lanthanides, and Pb and Bi could be removed. With two subsequent elutions, alkali and alkaline earth metals, lanthanides, actinides, and Zr and Nb could be removed. It was then estimated that the contaminating activity in the final  $^{90}\text{Sr}$ - $^{90}\text{Y}$  mixture should not exceed  $10^{-11}$  relative to the  $^{90}\text{Y}$  disintegration.<sup>22, 23</sup>

### B. Detectors and Shielding Geometry

The experimental arrangement is shown in Fig. 2. The evaporation residue of the purified  $^{90}\text{Sr}$  solution was buried at the center of a plastic phosphor cylinder (25-mm-diam by 25-mm-high NE-104) through a 2-mm-diam hole, drilled along the axis of a cylinder. The source strength was about 5  $\mu\text{Ci}$ . The  $\beta$  rays from  $^{90}\text{Y}$  were detected by this phosphor. The detector size was chosen so that its thickness is sufficient to stop the  $\beta$  rays of 2.26 MeV when the source was placed at the center of the plastic phosphor. The detector size and source position thus chosen have three advantages; that is, to reduce the external bremsstrahlung background due to the main branch from  $^{90}\text{Y}$ , to increase the solid angle at the source subtended by the detector, and to improve the  $\beta$  spectra. The plastic phosphor was mounted on an RCA-6810A photomultiplier tube through an 85-mm-long Lucite light-guide pipe having the same diameter as the phosphor.

Two 127-mm-diam by 50-mm-high NaI(Tl) crystals coupled to RCA-4522 phototubes were employed as the  $\gamma$ -ray detectors. In order to observe the two-photon decay with a very small probability, it was essential to get a large solid angle by positioning the detectors in an optimum direction. The two  $\gamma$ -ray detectors were placed at  $180^\circ$  to each other, 62 mm apart, by taking into account that the angular correlation function is  $1 + \cos^2\theta$ , assuming virtual occupation of the  $1^-$  states. The two detectors were aligned in the north-south direction. The front face of each  $\gamma$ -ray detector was set at 31 mm from the source. A special precaution was paid for the optical coupling by silicone oil between the phototube and the scintillator so as to achieve the unchanged condition during a long experimental period of more than three years. Two detectors were covered with 3-mm-thick polyethylene caps which serve as insulators for negative high voltages applied to the phototubes. These polyethylene caps were also used as electron absorbers.

A conical lead collimator between two  $\gamma$ -ray detectors was placed to minimize the Compton back-scattering from one detector to the other. The plastic phosphor having the  $^{90}\text{Sr}$  source was centered in the whole detector assembly through a 30-mm-diam hole, drilled on this conical collima-

tor vertically. In order to observe the very weak intensity of the two-photon decay, background contributions to the observed sum spectrum have to be considered. Without shielding of the detectors, the gated background sum spectrum obtained by preliminary experiments showed a small peak in the 1.76-MeV region. The detectors were then covered with a 50-mm-thick lead ring. Furthermore, three detectors including this 50-mm lead ring were housed in a 100-mm-thick lead shield, as shown in Fig. 2. In this fashion, a careful search was made for any peak in the 1.76-MeV region of the gated background sum spectrum measured prior to the main experimental runs. None was found in the region of interest. From these facts, this peak was interpreted as being mainly due to the  $\gamma$  rays originated from cosmic rays and/or natural activities in the room. It was also concluded that the contribution to the 1.76-MeV region from natural radioactivity, such as uranium and thorium decay species existing in the lead shields was negligibly small in this experiment.

To reduce gain drifts due to the temperature-dependent characteristics of the crystals and the phototubes, the whole detector assembly with lead shieldings was housed completely in a constant temperature chamber; the temperature was maintained at  $24 \pm 1^\circ\text{C}$  in duration of more than three years.

### C. Electronics

Since the sum of the energies of two  $\gamma$  rays in the two-photon decay is equal to the total transition energy, the use of a sum-coincidence technique is quite suited to this kind of experiment.

In Fig. 3 is shown the block diagram of the improved sum-coincidence spectrometer including an anticoincidence device using a  $\beta$ -ray detector. The EG & G fast circuits were used for the most parts of the present electronics arrangement. Fast signals from each NaI(Tl) detector were fed to a fast coincidence circuit (FCC) through two constant fraction-timing discriminators<sup>24</sup> set at 200 keV. In order to obtain high resolving time and high efficiency for both the FCC and the fast anticoincidence circuit (FAC), we employed the constant fraction-timing discriminators constructed in our laboratory. This circuit was designed specially for timing with the slow pulses from a NaI(Tl) detector by adopting a lower level discriminator with a self-resetter. The input pulse was set at 20% of full height. The resolving time of the FCC thus obtained was 11 nsec with a 100% coincidence efficiency for all coincident photon pairs with energies higher than 200 keV. The output signals from the FCC were fed to a "signal" input of the FAC having a resolving time of 13 nsec with an

efficiency of 100%. All  $\beta$  rays from the  $^{90}\text{Sr}$ - $^{90}\text{Y}$  source were detected by the plastic phosphor. The signals from the  $\beta$ -ray detector were led to a fast single-channel differential discriminator (FSD), which could respond to fast pulses from the plastic detector. The FSD was adjusted so as to accept all  $\beta$  pulses corresponding to energies between  $\sim 50$  and  $\sim 510$  keV of the weak  $\beta$  branch to the 1.76-MeV  $0^+$  state in  $^{90}\text{Zr}$ . One of the output branches of the FSD was used as an "antisignal" of the FAC to eliminate unfavorable coincident events, which were due to the Compton backscattering of the bremsstrahlung produced by the high-energy  $\beta$  rays, going from one  $\gamma$ -ray detector to the other, and due to double internal bremsstrahlung<sup>25, 26</sup> (two photons are created in the electric field of the nucleus during the  $\beta$  decay). At the same time, a small portion of the wanted pulses from the FCC were lost within the resolving time of the FAC, but most of these pulses ( $\sim 85\%$ , as the half-life of the 1.76-MeV  $0^+$  state is 62 nsec), not coincident with the signals from the  $\beta$ -ray detector in the FAC, could be routed to one of the channels of the first slow-coincidence circuit (SC-I) with coincidence resolution of 140 nsec. The other channel of the SC-I was fed by the energy-selected  $\beta$  pulses from the other output branch of the FSD. In SC-I, a narrow pulse (10 nsec wide) from the FAC was

set at the leading edge of a wide pulse (130 nsec wide) from the FSD. By employing the FAC the output counting rate of this SC-I was reduced by a factor 4. This implies that the unfavorable coincidence background can be reduced to the same extent. The SC-I made it possible to eliminate unfavorable coincident events detected by only two  $\gamma$ -ray detectors without triggering the  $\beta$ -ray detector. Only true coincident pulses corresponding to the two-photon decay were thus ascertained. A discussion on the possible sources of unfavorable coincidences is given in the following section.

The pulses from the tenth inner dynode of each RCA-4522  $\gamma$ -ray phototube were added in a linear summing circuit, and the outputs from this circuit, i.e., the sum spectrum to be studied, were analyzed in the first multichannel pulse-height analyzer (MPHA-I) by gating pulses sent from SC-I.

Measurements for the energy distribution of the two-photon decay were performed by observing the energy spectrum representing only fully absorbed energy of  $\gamma$  rays, in which the pulses due to the Compton scattering were completely excluded. The added pulses from a linear summing circuit were selected at the 1.76-MeV region by a single-channel differential discriminator (SD). To reduce the background component in the fully absorbed  $\gamma$ -ray spectrum, the second slow coincidence circuit (SC-II) was placed between this SD and the other output branch of the SC-I. The linear pulses from one of the  $\gamma$ -ray detectors were sent independently to the second amplifier through an attenuator, and recorded in the second multichannel pulse-height analyzer (MPHA-II) by gating pulses supplied by the SC-II (the photopeak method). Thus, the obtained pulse-height spectrum due to the fully absorbed energy (the photopeak spectrum) shows the energy distribution of one of two  $\gamma$  rays from the two-photon decay.

### III. MEASUREMENT AND RESULTS

Since data were accumulated for 1000 h, special precautions were made for stability of the circuit functions. Possible sources of unfavorable coincidences which might affect the observed sum spectrum and photopeak spectrum are discussed. The experimental results are analyzed in this section.

#### A. Measurements

First, the measurements of gated-total-sum spectrum and gated-total-photopeak spectrum, and of gated-random-sum spectrum and gated-random-photopeak spectrum were performed. Since coincidence counting rates were quite small, data were accumulated for 1000 h in each line. A line consists of ten 100-h runs, permuting the total

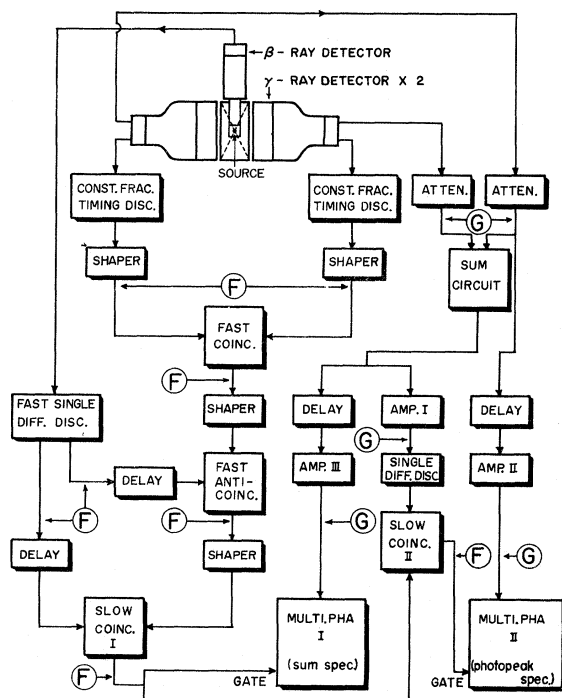


FIG. 3. Block diagram of the electronics. F and G designations are check points of electronics function and calibration points of the gain, respectively.

measurements and the random measurements every 100 h. For the convenience of the measurements, finally, measurements of gated-background-sum spectrum and gated-background-photopeak spectrum without source were made for 1000 h, also consisting of ten 100-h runs.

In all the present experiment the energy calibration was made every 100 h using a weak  $^{22}\text{Na}$  source inserted near the center of the detector assembly through the conical collimator while keeping the  $^{90}\text{Sr}$  source in the plastic phosphor. Circuit functions were also inspected carefully every 100 h with the  $^{90}\text{Sr}$  source in position but without the  $^{22}\text{Na}$  source; functions and gains of circuits were checked at the points indicated by F and G, respectively, shown in Fig. 3. The single  $\gamma$ -ray spectrum of  $^{22}\text{Na}$  by the NaI(Tl) detector shows the peaks of 0.511-MeV annihilation  $\gamma$  rays and 1.28-MeV nuclear radiation. However, the gated-sum spectrum obtained with the whole electronic equipment in position gives calibration peaks at 1.02, 1.79, and 2.30 MeV, while the ungated-sum spectrum from the linear summing circuit gives peaks at 0.511, 1.02, 1.28, 1.79, and 2.30 MeV.

Since in the use of a sum-coincidence spectrometer it is required that the calibration of energy should be identical for the two channels, the gains of the two phototubes were adjusted by corresponding attenuators so that the 0.511- and 1.28-MeV  $\gamma$ -ray peaks of  $^{22}\text{Na}$  from both detectors appeared in the same channels on the MPHA-I, keeping the summing circuit, delay box, and third amplifier in position. For the measurement of the photopeak spectrum, the pulse height corresponding to 1.76 MeV from the  $0^+$  state in  $^{90}\text{Zr}$  must be precisely selected in the SD. Therefore, energy selection at 1.76-MeV region was carefully made by this SD using five calibration peaks of  $^{22}\text{Na}$ , obtained by scanning the same SD.

Counting rates and coincidence counting rates at F's in Fig. 3 were constant within statistical fluctuation through the whole course of the experiment. On the other hand, when any gain drift, even only one channel in the MPHA-I was found, we abandoned the observed data obtained in a 100-h run prior to the check time.

The sum spectrum and the photopeak spectrum could be obtained simultaneously by our electronics arrangement. The experimental results are shown in Figs. 4-6. The 1.02-MeV sum peak by the annihilation radiation due to the internal-pair creation recorded simultaneously in the measurement of the gated total sum spectrum, shown in Fig. 4 (a), was used as an intensity reference. A 1.46-MeV sum peak, which was unexpectedly observed in the present electronics arrangement, may be interpreted as follows. The 1.46-MeV  $\gamma$  rays from  $^{40}\text{K}$

in the glass of the NaI(Tl) crystal window and of the photomultiplier tube head, are scattered by one NaI(Tl) crystal, its energy being absorbed in part. Upon reaching the other NaI(Tl) crystal, the rest of the energy of the scattered  $\gamma$  rays is completely absorbed. In the linear summing circuit, such scattering results in linear pulses corresponding to the energy of 1.46 MeV. These pulses were recorded in MPHA-I by gating pulses from the SC-I. These gating pulses are produced in such a way that the output pulses from the FAC caused by the self-coincidence of the scattered 1.46-MeV  $\gamma$  rays randomly coincided with a large number of the pulses from the  $\beta$ -ray detector in the SC-I.

The gated-random-sum spectrum was recorded by inserting a 250-nsec delay line in the output line of the FAC circuit. Since the 1.46-MeV peak occurs independently of the source, the number of counts under the 1.46-MeV peak in the gated-random-sum spectrum should be observed to the same degree as those under the gated-total-sum spectrum, as is seen in Fig. 4 (b). In the gated-random-sum spectrum one can also discern the peak at 1.02 MeV, which occurs for the same reason as the 1.46-MeV peak.

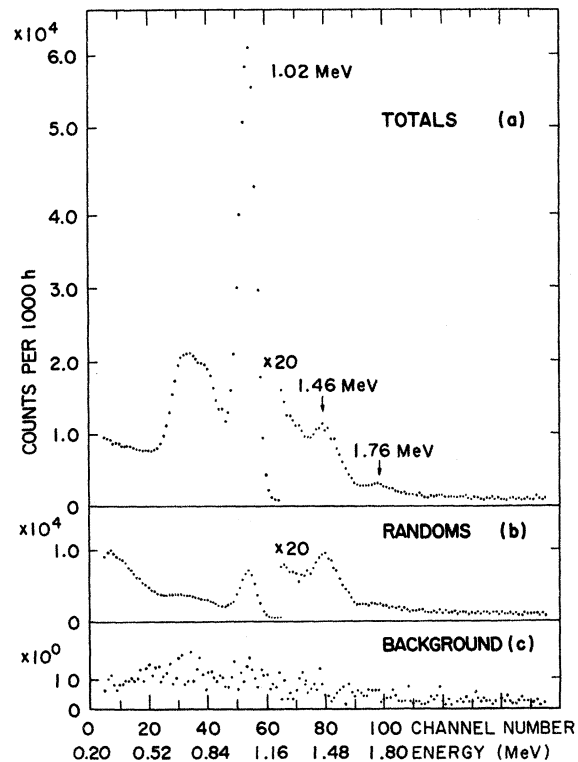


FIG. 4. (a) Gated-total-sum spectrum. (b) Gated-random-sum spectrum. (c) Gated-background-sum spectrum. Three peaks in the spectrum (a) and two peaks in the spectrum (b) are discussed in the text.

In Fig. 4 (c) is shown the gated-background-sum spectrum without the source but with a plastic dummy detector of the same size, the other detectors, and the shielding geometry in the same position as in the main experiments. No detectable peaks especially over the 1.76-MeV region were observed in scanning the entire spectrum. Because of the absence of a large number of pulses in the antichannel, the 1.46-MeV peak of  $^{40}\text{K}$  could not appear in this spectrum.

In order to obtain the net sum spectrum due to the two-photon decay, the gated random and background-sum spectra have been subtracted from the gated-total-sum spectrum. The result is shown in Fig. 5, where we drew the most reasonable background curve by best fitting an exponential function to the experimental points, except those in the region of interest, using a computer. The line profile of the 1.76-MeV peak is drawn as the most probable one by taking into account the energy resolution of the sum spectrum in this energy region.

The photopeak spectra were simultaneously recorded in MPHA-II. In the measurements of the gated-random-photopeak spectrum, an additional 250-nsec delay line was inserted in the output line of the SD placed in the sum channel. The gated-background-photopeak spectrum without the source was negligibly small. In Fig. 6 is shown a net photopeak spectrum obtained by subtracting the random photopeak spectrum from the total-photopeak spectrum. The number of counts under the peak of this spectrum should be the same as that of the sum spectrum. In the present measurement, however, the total counts of the photopeak spectrum were small compared with those of the sum peak because of narrow selection of the 1.76-MeV pulses in the SD.

#### B. Possible Sources of Errors

In evaluating the result thus obtained, the follow-

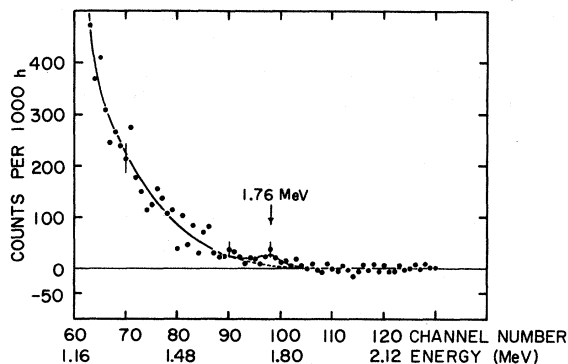


FIG. 5. Net spectrum of the 1.76-MeV region. This spectrum was obtained by subtracting randoms and background. The errors are standard deviations.

ing considerations were made. Possible sources of unfavorable coincidences, which could give rise to a peak at 1.76 MeV and to continuous distributions in the region of interest, may be classified as follows:

(a) A Compton backscattering from one NaI(Tl) crystal to the other for the intense bremsstrahlung (internal and external) produced in the  $\beta$  decay having the 2.26-MeV maximum energy. It should show a continuous distribution in this experimental condition.<sup>27</sup>

(b) Double internal bremsstrahlung produced in the  $\beta$  decay mentioned above. It should display a continuous spectrum.

(c) Contributions of cosmic radiations, natural radioactivity in the room and surroundings near the detectors, and radioactive impurities in the source. These have a chance to construct a peak at the 1.76 MeV.

Possible source (a) was extensively reduced by the use of the conical lead collimator between two  $\gamma$ -ray detectors. Since it is regarded that emission of  $\beta$  rays and the scattering of the bremsstrahlung created by them occur simultaneously, the remaining part of the scattered bremsstrahlung, which is not absorbed by the conical collimator, was removed by means of the FAC. In case (b), as the  $\beta$  rays and their double internal bremsstrahlung are also in time coincidence, unfavorable coincidences due to the double bremsstrahlung were also removed by our electronics. In case (c) the behavior of cosmic radiations and natural radioactivity in the room and surroundings near the detectors were critical in the present experiment, but contributions of these were removed by employing sufficiently thick lead shields, as described in the Sec. II. The contaminating impurities in the source were determined to be less than  $10^{-11}$  relative to the  $^{90}\text{Sr}$ - $^{90}\text{Y}$  disintegration. If the source contains impurities which emit  $\gamma$  rays with energies near the 1.76 MeV, serious error may result. A careful search was made for activities having these conditions through the whole Periodic Table. The conditions are fulfilled in the decay of  $^{214}\text{Bi}$

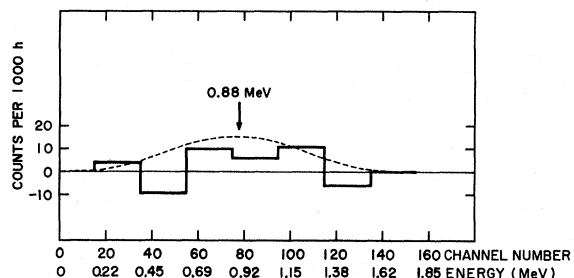


FIG. 6. Net photopeak spectrum. The dashed curve represents the theoretical curve  $W(\omega) \propto \omega^3(\omega_0 - \omega)^3$ .

(1.76-MeV  $\gamma$  rays),  $^{207}\text{Bi}$  (1.77-MeV  $\gamma$  rays), and  $^{212}\text{Bi}$  (1.8- and 1.64-MeV  $\gamma$  rays). It is postulated that the half-lives of the levels emitting  $\gamma$  rays from these nuclei are less than  $10^{-10}$  sec. Even if these nuclei exist in the source, the possible sources of error could be removed by our detector-electronics system. Thus, it was concluded that no disturbing effects from these possible sources of errors could be found at the 1.76-MeV region.

### C. Data Analysis

Thus, we conclude that in the end of the high energy tail of the 1.02-MeV peak in the spectrum shown in Fig. 5, a discernible peak at the 1.76-MeV energy is ascertained as to be from the  $0^+ \rightarrow 0^+$  transition in  $^{90}\text{Zr}$ . An independent series of the 1000-h measurements have resulted in the same forms as those shown in Figs. 4 and 5.

The ratio for the two-photon decay with respect to the sum of internal-pair and internal-conversion decay is given by the following expression:

$$\frac{T_{\gamma\gamma}}{T_{\pi+e}} = \frac{N_{\gamma\gamma}}{N_{\pi}(1+R)} \frac{\Omega \epsilon_{\pi}^2 a_{\pi}}{\Omega^2 \epsilon_{\gamma\gamma} a_{\gamma\gamma}} \frac{1}{FC(\theta)}. \quad (2)$$

The symbols in the expression are:

$T_{\gamma\gamma}$  = the probability for two-photon decay from the 1.76-MeV  $0^+$  state of  $^{90}\text{Zr}$ .

$T_{\pi+e}$  = the sum of the probability for internal-pair decay and that for internal-conversion decay.

$N_{\gamma\gamma}$  = the number of two-photon decays obtained from the sum peak per unit time.

$N_{\pi}$  = the number of observed pairs of annihilation quanta, which is proportional to the number of internal-pair decays per unit time.

$R$  = the ratio of the probability for internal-conversion decay to that for internal-pair decay.

$\Omega$  = the solid angle at the source subtended by the NaI(Tl) detector; the same for each detector.

$\epsilon_{\pi}$  = the photopeak efficiency for the 0.511-MeV  $\gamma$  rays due to two-photon annihilation created as a result of internal-pair creation.

$\epsilon_{\gamma\gamma}$  = the photopeak efficiency for the  $\gamma$ -ray pairs emitted in the two-photon decay, which is calculated from

$$\epsilon_{\gamma\gamma} = \frac{\int_0^{\omega_0} \epsilon(\omega) \epsilon(\omega_0 - \omega) W(\omega) d\omega}{\int_0^{\omega_0} W(\omega) d\omega}, \quad (3)$$

where notations are the same as those introduced in Sec. I.  $\epsilon(\omega)$  is the photopeak efficiency expressed by a function of  $\gamma$ -ray energy  $\omega$ .

$a_{\pi}$  = the correction factor for absorption of annihilation pairs in the plastic phosphor.

$a_{\gamma\gamma}$  = the correction factor for absorption of two  $\gamma$  rays in the plastic phosphor.

$F$  = the fraction of the energy spectrum of the two-photon decay which is accepted by the present electronic equipment.

$C(\theta)$  = the correction for finite detector solid angle, taking into account the angular correlation between two  $\gamma$  rays,  $(1 + \cos^2\theta)$ .

$N_{\gamma\gamma}$ , the number of counts under the 1.76-MeV sum peak in Fig. 5 was obtained as  $0.09 \pm 0.04$  per hour. The error given was evaluated from counting statistics and uncertainty in determining the shape of the high-energy tail of the 1.02-MeV peak distributed under the observed 1.76-MeV peak. As all positrons due to the internal-pair creation will completely annihilate in the source and plastic phosphor, the intensity of internal-pair decay is obtained from the number of 0.511-MeV coincidences. Annihilation pairs from the external-pair creation produced by the bremsstrahlung due to intense  $\beta$  rays were removed by the electronics we used. The quantity  $N_{\pi}$ , the number of counts under the 1.02-MeV sum peak in Fig. 5 was  $(3.47 \pm 0.01) \times 10^2$  per hour. As a value of  $R$ , we used an experimental value of  $2.38 \pm 0.08$  obtained by Nessin, Kruse, and Eklund.<sup>20</sup> The solid angle  $\Omega$  was  $(28 \pm 1.4)\%$  of  $4\pi$ . Since the annihilation photons are emitted exactly in the opposite directions, the geometrical efficiency for the 0.511-MeV pairs was taken as  $\Omega$  for two detectors, as is seen in a numerator of the second factor in the right-hand side of Eq. (2). The values of  $\epsilon_{\pi}$  and  $\epsilon_{\gamma\gamma}$  were computed to be  $0.46 \pm 0.02$  and  $0.099 \pm 0.005$ , respectively, using the FACOM 230-60 computer at Data Processing Center, Kyoto University. The value of  $a_{\pi}$  was computed to be  $0.68 \pm 0.02$ . In computing the value of  $a_{\gamma\gamma}$ , an energy of  $\gamma$  rays to be absorbed was used at a value of  $\frac{1}{2}\omega_0 = 0.88$  MeV. This value obtained was  $a_{\gamma\gamma} = 0.74 \pm 0.02$ . Energy selections in the two constant fraction-timing discriminators were considered in estimating the value of  $F = 0.95 \pm 0.05$ .  $C(\theta)$  was computed to be  $1.12 \pm 0.06$  taking into account finite detector solid angle for the angular correlation of two photons. By inserting these numerical values into Eq. (2), we obtain the final experimental value

$$\frac{T_{\gamma\gamma}}{T_{\pi+e}} = (5.1 \pm 2.5) \times 10^{-4}. \quad (4)$$

The experimental error comes mainly from an uncertainty in evaluating  $N_{\gamma\gamma}$ .

## IV. DISCUSSION

The photopeak spectrum shown in Fig. 6, though the statistics is poor, first reveals the shape of the energy distribution of two-photon decay. This spectrum indicates that the energy distribution of two-photon decay has a maximum intensity in the

0.88-MeV energy region, dropping off rapidly in both sides. The theoretical curve  $W(\omega) \propto \omega^3(\omega_0 - \omega)^3$ , was drawn by a dashed line for the sake of comparison. Reflecting the fact that the giant-dipole states at  $\sim 17$  MeV in  $^{90}\text{Zr}$  have been confirmed experimentally,<sup>28</sup> it is reasonable to favor that most acceptable multipolarity in two-photon decay of  $^{90}\text{Zr}$  is an ( $E1, E1$ ) type.

The experimental values of  $T_{\gamma\gamma}/T_{\pi+e}$  for  $^{90}\text{Zr}$  so far reported lie scattered in the wide range from  $2.3 \times 10^{-3}$  to  $8 \times 10^{-5}$ , as listed in Table I. All attempts appear to have led to ambiguous results. Previous workers applied no special precautions to one or more of the unfavorable effects described in Sec. III B.

The value obtained in the present work,  $(5.1 \pm 2.5) \times 10^{-4}$ , is larger than the upper limit recently reported,  $1.2 \times 10^{-4}$  by Vanderleeden and Jastram,<sup>18</sup> and  $1.8 \times 10^{-4}$  by Harihar, Ullman, and Wu.<sup>19, 29</sup> Even if we use  $R=3.0$ , which was measured by Yuasa, Laberrigue-Frolow, and Feuvrais,<sup>30</sup> instead of  $R=2.38$  adopted in the present work, the ratio  $T_{\gamma\gamma}/T_{\pi+e}$  becomes  $4.0 \times 10^{-4}$ . Measurements have been performed by Vanderleeden and Jastram using a two-dimensional pulse-height analyzer. Their result  $1.2 \times 10^{-4}$  involves uncertainties because of the presence of the obvious peak at the position just below the region of interest, which was explained by them to be instrumental in origin, and no precautions for the possible causes of unfavorable coincidences were made except for use of the conical collimator and sufficient thickness of the lead shields. Harihar, Ullman, and Wu have carefully investigated with the conical collimator and sufficient lead shielding for the detector system but with only sum-coincidence technique. In the sum spectrum obtained by them a discernible peak was observed in the energy region of 1.76 MeV. However, due to the insufficient statistics and no supporting evidence for the en-

ergy distribution and angular correlation of the pairs of  $\gamma$  rays in that sum-energy region, they refrained from proclaiming this peak as a definite observation of the two-photon decay. Our experimental technique having the advantage of being able to exclude disturbing effects and observe simultaneously the energy distribution of the two-photon decay may allow us to accept our value, although with a considerable error, as a reasonable value of  $T_{\gamma\gamma}/T_{\pi+e}$ .

The theoretical treatments to estimate the probability of two-photon decay in  $^{90}\text{Zr}$  have been made by a few workers. The single-particle model was used by Grechukhin,<sup>4, 8</sup> who obtained the value of  $T_{\gamma\gamma}/T_{\pi+e} = 2 \times 10^{-3}$ . The nuclear reaction theory used by Margolis<sup>10</sup> led to the value of  $6 \times 10^{-3}$ . The shell-model treatment of Yoccoz,<sup>11</sup> gave a value of  $1.6 \times 10^{-4}$  (quoted in Ref. 15) using  $1g_{9/2}$  and  $2p_{1/2}$  configurations for two  $0^+$  states, which were proposed by Talmi and Unna.<sup>31</sup> If the giant-dipole states lie sufficiently above the first excited state, the probability for the two-photon decay can be described independently of the matrix elements in the transitions between the giant-dipole states and low-lying states.<sup>8</sup> Since the probability for this process is expected to be small, as in all the second-order processes, the experimental value of the probability hence may provide a severe test of any nuclear model for a description of the two  $0^+$  states. Our result is larger than the shell-model calculation given by Yoccoz. The value obtained in the present work calls upon more refined calculations for the probability of two-photon decay using the other shell-models, such as the treatments of Bertsch,<sup>32</sup> and Brown and Green,<sup>33</sup> who well explain the deformed rotational nature of the excited states of  $^{16}\text{O}$ , or some other models.

Although the experimental method we employed has the advantage of excluding many causes of unfavorable coincidences, it must be admitted that

TABLE I. Experimental results on two-photon decay of the 1.76-MeV  $0^+$  first excited state to the  $0^+$  ground state in  $^{90}\text{Zr}$ .

$T_{\gamma\gamma}/T_{\pi+e}$	Worker(s)	Reference
$= (2.3 \pm 1.5) \times 10^{-3}$	Langhoff and Hennies (1961)	12
$= 1.1 \times 10^{-3}$	Ryde, Thieberger, and Alväger (1961)	13 <sup>a</sup>
$\leq 1.4 \times 10^{-3}$	Gorodetzky <i>et al.</i> (1961)	14
$\leq 6.4 \times 10^{-4}$	Sutter (1963)	15
$< 4.2 \times 10^{-4}$	Ryde (1963)	16 <sup>a</sup>
$\leq 8 \times 10^{-5}$	Vanderleeden and Jastram (1965)	17
$\leq 1.2 \times 10^{-4}$	Vanderleeden and Jastram (1970)	18
$\leq 1.8 \times 10^{-4}$	Harihar, Ullman, and Wu (1970)	19
$= (5.1 \pm 2.5) \times 10^{-4}$	Present work	

<sup>a</sup> The original result is shown in the form of  $T_{\gamma\gamma}/T_e$ , from which the value of  $T_{\gamma\gamma}/T_{\pi+e}$  is reduced using the relation  $T_e/T_{\pi} = 2.38$ .



this method has the disadvantage of increasing the random coincidence peak of 1.46 MeV from  $^{40}\text{K}$  with increasing of the source strength. Consequently, the source strength to be used is restricted to 10  $\mu\text{Ci}$  at most. It is hoped that more accu-

rate measurements for the two-photon branching ratio can be carried out by means of further improved experimental methods, as well as the angular correlation between two  $\gamma$  rays can be observed.

#### ACKNOWLEDGMENTS

The author would like to express his deep appreciation to Professor Sakae Shimizu for his stimulating discussions and kind encouragement during the long course of this work. He also wishes to thank Dr. Mutsuo Koyama of the Department of Chemistry, Kyoto University for his invaluable help with the purification of the  $^{90}\text{Sr}$  source. Thanks are further due to Dr. Yasuhito Isozumi for his assistance throughout all phases of this study, Dr. Takeshi Mukoyama for his assistance in the use of the computer programming, and Shoji Isozumi for his cooperation in making the constant fraction-timing discriminators.

- 
- <sup>1</sup>J. R. Oppenheimer and J. S. Schwinger, *Phys. Rev.* **56**, 1066 (1939).  
<sup>2</sup>R. G. Sachs, *Phys. Rev.* **57**, 194 (1940).  
<sup>3</sup>M. L. Goldberger, *Phys. Rev.* **73**, 1119 (1948).  
<sup>4</sup>D. P. Grechukhin, *Zh. Eksperim. i Teor. Fiz.* **32**, 1036 (1957) [transl.: *Soviet Phys. - JETP* **5**, 846 (1957)].  
<sup>5</sup>J. Eichler and G. Jacob, *Z. Physik* **157**, 286 (1959).  
<sup>6</sup>J. Eichler, *Z. Physik* **160**, 333 (1960).  
<sup>7</sup>D. P. Grechukhin, *Nucl. Phys.* **35**, 98 (1962).  
<sup>8</sup>D. P. Grechukhin, *Nucl. Phys.* **47**, 273 (1963).  
<sup>9</sup>D. P. Grechukhin, *Nucl. Phys.* **62**, 273 (1965).  
<sup>10</sup>B. Margolis, *Nucl. Phys.* **28**, 524 (1961).  
<sup>11</sup>J. Yoccoz, *J. Phys. Radium* **22**, 685 (1961).  
<sup>12</sup>H. Langhoff and H. H. Hennies, *Z. Physik* **164**, 166 (1961).  
<sup>13</sup>H. Ryde, P. Thieberger, and T. Alväger, *Phys. Rev. Letters* **6**, 475 (1961).  
<sup>14</sup>S. Gorodetzky, G. Sutter, R. Armbruster, P. Chevalier, P. Mennrath, F. Scheibling, and J. Yoccoz, *J. Phys. Radium* **22**, 688 (1961).  
<sup>15</sup>G. Sutter, *Ann. Phys. (Paris)* **8**, 323 (1963).  
<sup>16</sup>H. Ryde, *Arkiv Fysik* **23**, 247 (1963).  
<sup>17</sup>J. C. Vanderleeden and P. S. Jastram, *Phys. Letters* **19**, 27 (1965).  
<sup>18</sup>J. C. Vanderleeden and P. S. Jastram, *Phys. Rev. C* **1**, 1025 (1970).  
<sup>19</sup>P. Harihar, J. D. Ullman, and C. S. Wu, *Phys. Rev. C* **2**, 462 (1970).  
<sup>20</sup>M. Nessim, T. H. Kruse, and K. E. Eklund, *Phys. Rev.* **125**, 639 (1962).  
<sup>21</sup>R. M. Kloepper, R. B. Day, and D. A. Lind, *Phys. Rev.* **114**, 240 (1959).  
<sup>22</sup>R. M. Diamond, K. Street, Jr., and G. T. Seaborg, *J. Am. Chem. Soc.* **76**, 1461 (1954).  
<sup>23</sup>W. E. Nervik, *J. Phys. Chem.* **59**, 690 (1955).  
<sup>24</sup>D. A. Gedcke and W. J. McDonald, *Nucl. Instr. Methods* **58**, 253 (1968).  
<sup>25</sup>J. E. Thun, W. D. Hamilton, K. Siegbahn, and K. E. Eriksson, *Arkiv Fysik* **22**, 565 (1962).  
<sup>26</sup>P. S. Jastram and J. C. Vanderleeden, *Phys. Rev. C* **1**, 1036 (1970).  
<sup>27</sup>The same effect due to  $\gamma$  rays from the single-quantum annihilation of positrons from the internal-pair decay of the transition concerned cannot be eliminated by our electronics. But this effect is negligibly small in the present case.  
<sup>28</sup>See, for example, A. Lepretre, H. Bell, R. Bergere, P. Carlos, A. Veysiere, and M. Sugawara, *Nucl. Phys.* **A175**, 609 (1971).  
<sup>29</sup>C. S. Wu, private communication: In Eq. (1) of their paper [Ref. 19]  $\Omega^2$  should be  $\Omega$ ; the exponent power 2 on  $\Omega$  was an error introduced in print setting.  
<sup>30</sup>T. Yuasa, J. Laberrigue-Frolow, and L. Feuvrais, *J. Phys. Radium* **18**, 498 (1957).  
<sup>31</sup>I. Talmi and I. Unna, *Nucl. Phys.* **19**, 225 (1960).  
<sup>32</sup>G. F. Bertsch, *Phys. Letters* **21**, 70 (1966).  
<sup>33</sup>G. E. Brown and A. M. Green, *Nucl. Phys.* **75**, 401 (1966).